

QUANTUM FIELDS FAR FROM EQUILIBRIUM AND THERMALIZATION

J. BERGES

*Institute for Theoretical Physics, University of Heidelberg,
Philosophenweg 16, 69120 Heidelberg, Germany
E-mail: j.berges@thphys.uni-heidelberg.de*

I review the use of the $2PI$ effective action in nonequilibrium quantum field theory. The approach enables one to find approximation schemes which circumvent longstanding problems of non-thermal or secular (unbounded) late-time evolutions encountered in standard loop or $1/N$ expansions of the $1PI$ effective action. It is shown that late-time thermalization can be described from a numerical solution of the three-loop $2PI$ effective action for a scalar ϕ^4 -theory in 1+1 dimensions (with Jürgen Cox, hep-ph/0006160). Quantitative results far from equilibrium beyond the weak coupling expansion can be obtained from the $1/N$ expansion of the $2PI$ effective action at next-to-leading order (NLO), calculated for a scalar $O(N)$ symmetric quantum field theory (hep-ph/0105311). Extending recent calculations in classical field theory by Aarts et al. (hep-ph/0007357) and by Blagoev et al. (hep-ph/0106195) to $N > 1$ we show that the NLO approximation converges to exact (MC) results already for moderate values of N (with Gert Aarts, hep-ph/0107129). I comment on characteristic time scales in scalar quantum field theory and the applicability of classical field theory for sufficiently high initial occupation numbers.

1 Introduction

Nonequilibrium dynamics of quantum fields is much less well understood than its thermal equilibrium limit. Important progress has been achieved for systems close to equilibrium, including (non)linear response techniques, gradient expansions or effective descriptions based on a separation of scales in the weak coupling limit¹. Current and upcoming heavy ion collision experiments provide an important motivation to find controlled approximation schemes which yield a quantitative description of **far-from-equilibrium** phenomena. Other applications include (p)reheating at the end of inflation in the early universe, the physics of baryogenesis or measurements of the dynamics of Bose-Einstein condensation.

To study nonequilibrium phenomena no other dynamics than the known Hamiltonian time-evolution of quantum fields is necessary. In particular, the observed macroscopic, effectively dissipative behavior or thermalization has to arise from the underlying reversible quantum dynamics. Addressing these questions one has to find approximation schemes which respect all symmetries of the underlying theory, such as time-reflection symmetry. Far from equilibrium the dynamics can involve very different length scales and a priori there

is typically no effective description based on a clear separation of scales which is valid at all times. Similarly, the relevant renormalized interactions between modes can become large at intermediate times and expansions based on weak coupling arguments are limited.

Here we report on recent progress to find suitable approximation schemes for far-from-equilibrium dynamics based on the two-particle irreducible ($2PI$) generating functional for Green's functions². The approach does not employ the loop expansion of the $2PI$ effective action relevant at weak couplings^{2,3}, and extends first calculations of late-time thermalization for quantum fields solving the three-loop $2PI$ approximation^{4,5}. To obtain a small nonperturbative expansion parameter for far-from-equilibrium dynamics we consider a systematic **$1/N$ expansion of the $2PI$ effective action**⁶. Since the truncation error may be controlled by higher powers of $1/N$ this expansion is not restricted to weak couplings or situations close to equilibrium. The next-to-leading order (NLO) approximation has been solved numerically for a scalar $O(N)$ symmetric quantum field theory in 1+1 dimensions^{6,7}. The $1/N$ expansion of the $2PI$ effective action in the NLO approximation is equivalent to the “BVA” approximation^a discussed earlier for quantum oscillators in Ref.⁸. Recently, this approximation has been studied for a one-component classical field theory in Ref.⁹ and compared with exact (MC) results by numerically integrating the classical evolution equations and sampling over initial conditions.²¹ Extending this analysis to the N -component classical $O(N)$ model one can show⁷ that the $1/N$ expansion at NLO yields systematically, by increasing N , quantitatively precise results already for moderate values of N .

Controlled computational methods for the approximative solution of non-equilibrium dynamics are limited so far. Leading order large- N or mean field type approximations neglect scattering and are known to fail to describe thermalization¹⁰. Standard (finite-loop) perturbative descriptions¹¹ or $1/N$ expansions of the generating functional for one-particle irreducible ($1PI$) Green's functions beyond leading order can be secular (unbounded) and break down at late times¹². It is known that the calculation of transport coefficients¹⁴ involves already an infinite series of diagrams not included at any finite order in the $1/N$ expansion of the $1PI$ effective action. In contrast, the relevant diagrams can be efficiently captured in finite-order loop¹⁵ or $1/N$ expansion⁶ at NLO and NNLO of the $2PI$ effective action. The three-loop order has been also frequently used as a starting point for kinetic descriptions and comprises the Boltzmann equation^{16,17,3,18,19,20}.

^aThe name “Bare-Vertex-Approximation” refers to an ansatz on the level of a specific Schwinger-Dyson equation⁸. Note that the four-vertex gets renormalized at next-to-leading order $2PI$ ⁶.

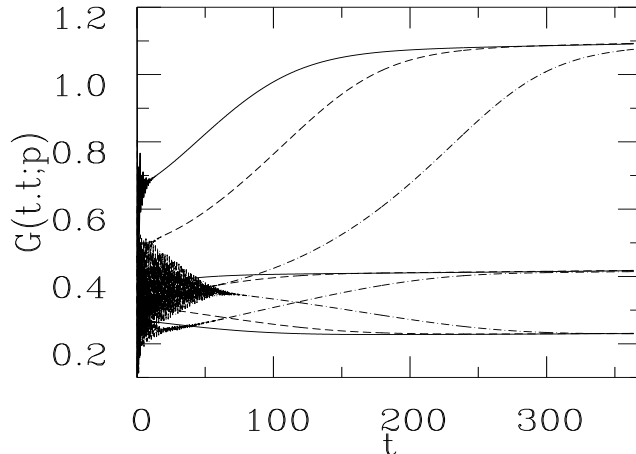


Figure 1: Examples for the time dependence of the equal-time propagator $G(t, t; \mathbf{p})$ with Fourier modes $|\mathbf{p}| = 0, 3, 5$ from a first $2PI$ three-loop solution⁴ (all in initial-time mass units). The evolution is shown for three very different initial conditions with the same average energy density. After an effective damping of rapid oscillations at early times the modes are still not close to equilibrium. It is followed by a smooth “drifting” of modes and a subsequent late-time approach to thermal equilibrium. The late-time behavior of the correlator modes is insensitive to the initial conditions and their value uniquely determined by the conserved energy density. This qualitative behavior has been verified beyond the loop/weak coupling expansion using the $(2PI)$ $1/N$ expansion at next-to-leading order⁶.

2 Thermal fixed point

We consider a scalar quantum field theory with action,

$$S = \int d^{d+1}x \left(\frac{1}{2} \partial_{x^0} \varphi_a \partial_{x^0} \varphi_a - \frac{1}{2} \partial_{\mathbf{x}} \varphi_a \partial_{\mathbf{x}} \varphi_a - \frac{1}{2} m^2 \varphi_a \varphi_a - \frac{\lambda}{4!N} (\varphi_a \varphi_a)^2 \right) \quad (1)$$

where $\varphi_a(x)$, $x \equiv (x^0, \mathbf{x})$, is a real, scalar field with $a = 1, \dots, N$ components. For $N = 4$ this corresponds to the linear sigma model for the light scalar and pseudoscalar pion degrees of freedom $(\sigma, \vec{\pi})$ respecting global chiral $O(4)$ symmetry, or to the Higgs sector of the electroweak standard model in absence of gauge field interactions. To save computational time the numerical results will be presented for $1+1$ dimensions. We stress that in the low dimensional theory many realistic questions cannot be addressed, in particular since there is no spontaneous symmetry breaking. The dynamics may help to understand the symmetric regime relevant for sufficiently high energy densities.

Before describing the nonequilibrium dynamics of this model in more detail below we give here an overview. As pointed out in Ref.⁴, for very different

nonequilibrium initial conditions a universal asymptotic late-time behavior of quantum fields can be observed. This behavior is demonstrated in Fig. 1 for the equal-time propagator $G(t, t; \mathbf{p})$ in the three-loop $2PI$ approximation as a function of time t for three Fourier modes, each starting from three very different initial conditions with the same average energy density. For the solid line the initial conditions are close to a mean field thermal solution, the initial mode distribution for the dashed and the dashed-dotted lines deviate more and more from thermal equilibrium⁴. It is striking to observe that propagator modes with very different initial values but with the same momentum \mathbf{p} approach the same large-time value^b. The late-time result approaches the equilibrium correlation modes of the corresponding thermal field theory⁴.

The observed real-time dynamics of correlator modes bears some similarities with a Wilsonian renormalization group flow of couplings towards an attractive fixed point. For the latter the large-distance or low-energy behavior near the fixed point is insensitive to details at short distances or high energies. For the real-time evolution we observe that the large-time behavior is insensitive to details at early times. The role of the fixed point is played here by a time-translation invariant solution for the correlators obeying the standard periodicity (KMS) condition for thermal equilibrium. Time translation invariant solutions play an important role for the late-time dynamics of nonequilibrium field theory. This fact is known as well for the leading order (LO) large- N or mean field type approximations^{22,23,24} which neglect scattering: At LO the correlator modes approach time-translation invariant solutions at asymptotically large times^{21,25,6}. Those leading order “fixed points”²⁶ are distinct from the thermal one. In particular, the LO fixed points depend explicitly on the initial particle number distribution, the simple reason being that the LO approximation exhibits an additional conserved quantity (particle number) which is not present in the full theory. The LO fixed points become unstable once scattering is taken into account and the system approaches the thermal fixed (cf. the detailed LO/NLO comparison in Ref.⁶). We emphasize that the described qualitative aspects are the same if we take into account scattering in the ($2PI$) three-loop or $1/N$ expansion at NLO, though quantitative aspects are different. We now go through the different characteristic time regimes in more detail using the $1/N$ expansion of the $2PI$ effective action at NLO, which provides for sufficiently large N a small nonperturbative expansion parameter.

^bWe emphasize that thermalization or independence of the initial conditions cannot be observed in a strict sense because of time-reversal invariance (note that thermal equilibrium is invariant under time translation and bears no information about initial conditions). Our results demonstrate that thermal equilibrium can be approached closely with time, indistinguishable for practical matters. It cannot reach it on a fundamental level without some kind of coarse graining which is a matter of principle and not a question of approximation.

3 Controlled nonperturbative approach

All correlation functions of the quantum theory can be obtained from the effective action $\Gamma[\phi, G]$, here the *2PI* generating functional for Green's functions, which is parametrized by the field $G_{ab}(x, y)$ representing the expectation value of the time ordered composite $T\varphi_a(x)\varphi_b(y)$ and the macroscopic field $\phi_a(x)$ given by the expectation value of $\varphi_a(x)$.² We will concentrate in the following on the symmetric regime where it is sufficient to consider $\Gamma[\phi = 0, G] \equiv \Gamma[G]$. The *2PI* generating functional for Green's functions can be parametrized as²

$$\Gamma[G] = \frac{i}{2}\text{Tr} \ln G^{-1} + \frac{i}{2}\text{Tr} G_0^{-1}G + \Gamma_2[G] + \text{const}, \quad (2)$$

where $G_0^{-1} = i(\square + m^2)$ denotes the free inverse propagator. Writing $\Gamma_2[G] = \Gamma_2^{\text{LO}}[G] + \Gamma_2^{\text{NLO}}[G] + \dots$ the LO and NLO contributions are given by^{6,8}

$$\Gamma_2^{\text{LO}}[G] = -\frac{\lambda}{4!N} \int_{\mathcal{C}} d^{d+1}x G_{aa}(x, x)G_{bb}(x, x), \quad (3)$$

$$\Gamma_2^{\text{NLO}}[G] = \frac{i}{2} \int_{\mathcal{C}} d^{d+1}x \ln[\mathbf{B}(G)](x, x). \quad (4)$$

Here \mathcal{C} denotes the Schwinger-Keldysh contour along the real time axis²⁷ and

$$\mathbf{B}(x, y; G) = \delta_{\mathcal{C}}^{d+1}(x - y) + i\frac{\lambda}{6N} G_{ab}(x, y)G_{ab}(x, y). \quad (5)$$

The nonlocal four-point vertex at NLO is given by $\frac{\lambda}{6N} \mathbf{B}^{-1}$.⁶ In absence of external sources the evolution equation for G is determined by²

$$\frac{\delta\Gamma[G]}{\delta G_{ab}(x, y)} = 0. \quad (6)$$

In the following we solve Eq. (6), using Eqs. (2)–(5) without further approximations numerically in 1 + 1 dimensions. For a detailed description of the approach, the numerical implementation and results see Ref.⁶. We present the results using the decomposition identity

$$G(x, y) = F(x, y) - (i/2)\rho(x, y) \text{sign}_{\mathcal{C}}(x^0 - y^0) \quad (7)$$

where F is the symmetric or statistical two-point function and ρ denotes the spectral function⁵. In thermal equilibrium F and ρ would be related by the fluctuation-dissipation theorem, however, far from equilibrium both two-point functions are linearly independent.

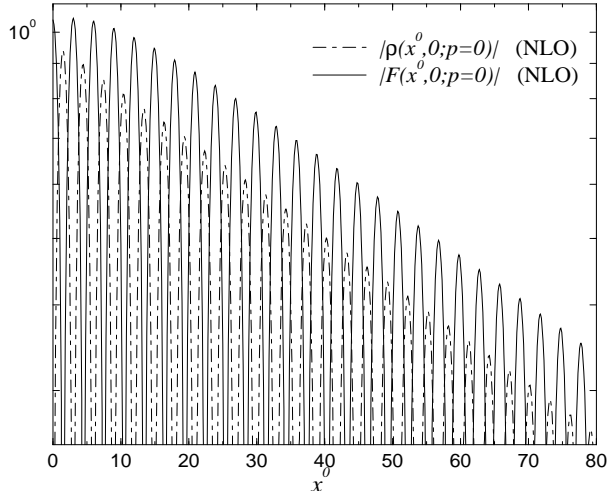


Figure 2: Logarithmic plot⁶ of the spectral and statistical two-point modes, $|\rho(x^0, 0; p = 0)|$ and $|F(x^0, 0; p = 0)|$ (in units of M_I). The correlation modes oscillations quickly approach an exponentially damped behavior with a corresponding characteristic time scale.

4 Early-time exponential damping

We study the time evolution for two classes of initial condition scenarios away from equilibrium. The first one corresponds to a “quench” where initially at high temperature one considers the relaxation processes following an instant “cooling” described by a sudden drop in the effective mass. The second scenario is characterized by initially Gaussian distributed modes in a narrow momentum range around $\pm p_{ts}$, which is reminiscent of colliding wave packets moving with opposite and equal momentum²⁸. A similar nonthermal and radially symmetric distribution of highly populated modes may also be encountered in a “color glass condensate” at saturated gluon density with typical momentum scale p_{ts} ²⁹.

We start with a quench from an initial high temperature particle number distribution $n_0(p) = 1/(\exp[\sqrt{p^2 + M_0^2}/T_0] - 1)$ with $T_0 = 2M_I$, $M_0^2 = 2M_I^2$ in units of the renormalized mass M_I at initial time $t = 0$, and a weak effective coupling $\lambda/6N = 0.083 M_I^2$ for $N = 10$. From Fig. 2 one observes that the statistical and spectral two-point functions, F and ρ , oscillate with initial frequency $\epsilon_0/2\pi = 0.17M_I$. The shown correlation functions quickly approach an exponentially damped behavior with characteristic rate $\gamma_0^{(\text{damp})} = 0.016M_I$. After the damping time scale $\tau^{(\text{damp})} \sim 1/\gamma_0^{(\text{damp})}$ correlations with initial times are effectively suppressed and asymptotically F and $\rho(t, 0; p) \rightarrow 0^+$.

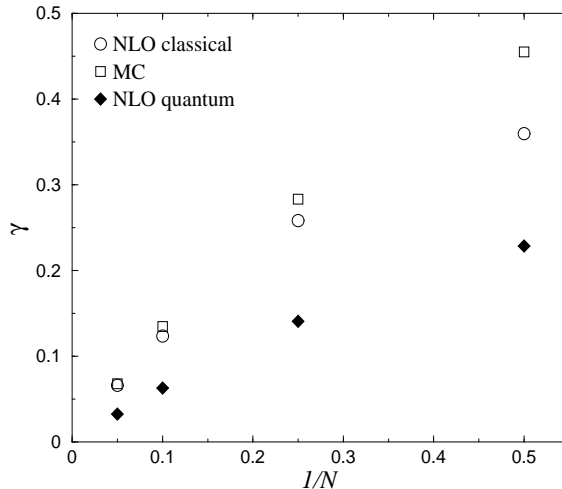


Figure 3: Nonequilibrium damping rates extracted from $F(t, 0; p = 0)$ as a function of $1/N$ for strong initial coupling $\lambda/M_I^2 = 30$. The quantum results are shown with full symbols. The damping rates are reduced compared to the classical field theory limit⁷ (open symbols). For the classical theory round symbols represent results from the next-to-leading order $1/N$ approximation and square ones denote the exact MC results. One observes a rapid convergence of the $1/N$ expansion at NLO to the exact result already for moderate values of N .

In Fig. 3 we show the damping rate as a function of $1/N$, this time for a strong initial coupling $\lambda/M_I^2 = 30$. The initial particle number $n_0(p)$ is chosen to represent a Gaussian distribution peaked around $p_{ts} = 2.5M_I$ with a thermal background of temperature $T_0 = 4M_I$ ^{6,7}. The full symbols show the NLO results for the quantum theory. One observes that the damping time $\sim 1/\gamma^{\text{damp}}$ scales proportional to N for sufficiently large N . It becomes apparent that LO ($N \rightarrow \infty$) or mean field type approximations fail to describe damping correctly and can be valid only for times $t \ll \tau^{(\text{damp})}$. To demonstrate the power of the (2PI) $1/N$ expansion we repeat the NLO calculation for the corresponding classical statistical field theory where comparison with exact (MC) results⁷, including all orders of $1/N$, is possible. The systematic convergence of the NLO and the Monte Carlo result is apparent from Fig. 3.

5 Non-exponential/power law drifting at intermediate times

After the characteristic early-time scale $\tau^{(\text{damp})} \sim 1/\gamma^{\text{damp}}$ the system is typically still far away from equilibrium for a relatively long time. For a large variety of initial conditions we find a subsequent parametrically slow, non-exponential “drifting” of modes, as exemplified in Fig. 1. To become more

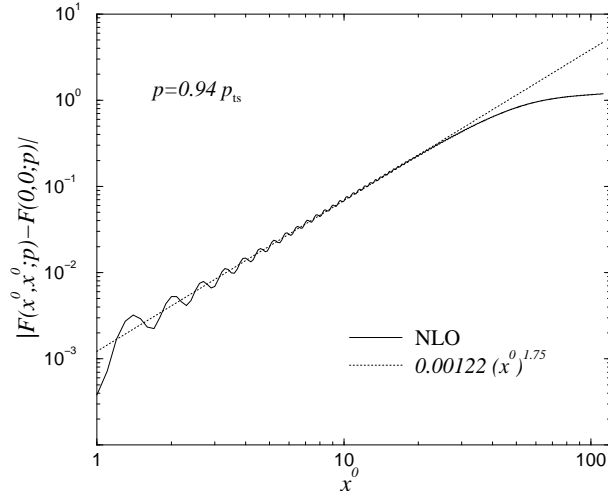


Figure 4: Double logarithmic plot⁶ for the equal-time mode $F(x^0, x^0; p)$ for an initial particle number distribution peaked around $p = p_{\text{ts}}$. The dotted straight line corresponds to a power law behavior $\sim (x^0 M_{\text{INIT}})^{1.75}$. At later times the behavior changes to an exponential approach to thermal equilibrium with rate $\gamma^{\text{therm}} \ll \gamma^{\text{damp}}$.

quantitative we show in Fig. 4 the statistical two-point function on a double logarithmic plot for a Gaussian initial particle number distribution similar to the one above and with small effective coupling $\lambda/6N = 0.1M_{\text{I}}^2$ for $N = 10$.⁶ Time-averaged over the oscillation period the evolution of the equal-time mode is well approximated by a power law behavior for times $t \lesssim 30/M_{\text{INIT}}$. The observed scaling behavior is reminiscent of a cascade in fully developed turbulence. However, note that the initial condition is homogeneous in space and all the energy is initially concentrated in a small momentum range. The energy has then to be distributed from the densely populated modes at high momentum in particular to the low momentum modes in order to reach thermal equilibrium. The presence of power law behavior at intermediate times can be observed for a variety of initial conditions. For higher n -point functions one can also observe approximate scaling, however, the detailed time evolution before the late-time thermalization can be rather complex and depends on the initial conditions. See Ref.⁶ for more details.

6 Late-time exponential thermalization

We emphasize that irrespective of the details of the initial conditions we find⁶ quite different rates for damping and for the late-time exponential approach to thermal equilibrium. For the example of Fig. 4 the characteristic time scales

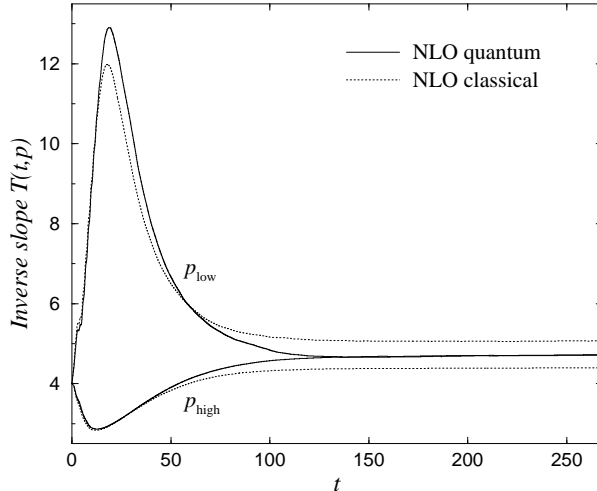


Figure 5: Time dependence of the inverse slope $T(t, p)$, as defined in the text^{7,6}. When quantum thermal equilibrium with a Bose-Einstein distributed particle number $n(t, \epsilon_p)$ is approached, all modes have to get equal $T(t, p) = T_{\text{eq}}$. In contrast, for classical thermal equilibrium the inverse slope is momentum dependent with $T(p_{\text{low}}) > T(p_{\text{high}})$.

$\gamma^{(\text{damp})}/\gamma^{(\text{therm})} \sim \mathcal{O}(10)$.^c Though the exponential damping at early times is crucial for an effective loss of details of the initial conditions — a prerequisite for the approach to equilibrium — it does not determine the time scale for thermalization. It is possible to relate the damping rate to the “width” of the Wigner transformed spectral function ρ in the same way as discussed in Ref. ⁵, however, the thermalization rate cannot. This fact may be particularly pronounced in 1+1 dimensions where on-shell two-to-two scattering is constrained by the energy conservation relation such that it does not change the particle numbers for the involved momentum modes. Processes with nontrivial momentum exchange are necessary for thermalization and are taken into account at NLO by off-shell effects. Correspondingly the calculation of the three-particle peak from off-shell decay of the nonequilibrium spectral function in Ref. ⁵ clearly shows a nonvanishing contribution. On-shell particle number changing processes appear at NNLO and may change quantitative aspects. The on-shell corrections beyond NLO are known to be small in the statistical field theory limit where exact results including all orders in $1/N$ show very good agreement with the NLO approximation already for moderate values of N .⁷

^cFor the employed spatially homogeneous initial conditions we do not observe a power-law “tail” for the late-time evolution. This behavior is insensitive to changes of large volumes.

The nontrivial fact that quantum thermal equilibrium is approached becomes more pronounced if one compares with classical²¹ thermalization. The classical field approximation is expected to become a reliable description for the quantum theory if the number of field quanta in each field mode is sufficiently high. Accordingly, we observe that increasing the initial particle number density leads to a convergence of quantum and classical time evolution⁷. However, since classical and quantum thermal equilibrium are distinct the respective evolutions have to deviate at sufficiently late times, irrespective of the initial particle number density. Differences in the particle number distribution can be conveniently discussed using the inverse slope parameter $T(t, p) \equiv -n(t, \epsilon_p)[n(t, \epsilon_p) + 1](dn/d\epsilon)^{-1}$ for a given time-evolving particle number distribution $n(t, \epsilon_p)$ and dispersion relation $\epsilon_p(t)$.⁶ Following Ref.⁵ we define the effective particle number as $n(t, \epsilon_p) + \frac{1}{2} \equiv [F(t, t'; p) \partial_t \partial_{t'} F(t, t'; p)]^{1/2}|_{t=t'}$ and mode energy by $\epsilon_p(t) \equiv [\partial_t \partial_{t'} F(t, t'; p) / F(t, t'; p)]^{1/2}|_{t=t'}$, which coincide with the usual free-field definition for $\lambda \rightarrow 0$. For a Bose-Einstein distributed particle number the parameter $T(t, p)$ corresponds to the (momentum independent) temperature $T(t, p) = T_{\text{eq}}$. In the classical limit the inverse slope $T(t, p)$ as defined above remains momentum dependent. In Fig. 5 we plot the function $T(t, p)$ for $p_{\text{low}} \simeq 0$ and $p_{\text{high}} \simeq 2p_{\text{ts}}$. Initially one observes a very different behavior of $T(t, p)$ for the low and high momentum modes, indicating that the system is far from equilibrium. Note that classical and quantum evolution agree very well for sufficiently high initial particle number density⁷. However, at later times the quantum evolution approaches quantum thermal equilibrium with a constant inverse slope $T = 4.7M_{\text{Pl}}$.⁶ In contrast, in the classical limit the slope parameter remains momentum dependent and the system relaxes towards classical thermal equilibrium⁷.

7 Conclusions

The $2PI$ effective action provides a powerful framework to find practicable approximations for nonequilibrium dynamics. Combined with a $(2PI)$ $1/N$ expansion beyond leading order one obtains a controlled nonperturbative description of far-from-equilibrium dynamics at early times as well as late-time thermalization. This includes the important capability of the $1/N$ expansion to describe nontrivial scaling properties near second order phase transitions at NLO and beyond. Most pressing is the extension to $3+1$ dimensions along the lines of Ref.⁶. This allows one to quantitatively address in a quantum field theory the formation of disoriented chiral condensates or fluctuations near critical points in the context of heavy-ion collisions, or of (p)reheating at the end of inflation in the early universe.

Acknowledgments

I thank my collaborators G. Aarts and J. Cox, and B. Müller for helpful discussions. Many thanks to the organizers of this very interesting workshop and for the invitation to give this talk.

References

1. For a review see D. Bödeker, Nucl. Phys. Proc. Suppl. **94** (2001) 61.
2. J. M. Cornwall, R. Jackiw, E. Tomboulis, Phys. Rev. **D10** (1974) 2428; see also J.M. Luttinger and J.C. Ward, Phys. Rev. **118** (1960) 1417; G. Baym, Phys. Rev. **127** (1962) 1391.
3. E. Calzetta, B. L. Hu, Phys. Rev. **D37** (1988) 2878; K. Chou, Z. Su, B. Hao and L. Yu, Phys. Rept. **118** (1985) 1.
4. J. Berges, J. Cox, Phys. Lett. **B** to appear [hep-ph/0006160].
5. G. Aarts, J. Berges, Phys. Rev. **D64** (2001) 0850XX [hep-ph/0103049].
6. J. Berges, Nucl. Phys. **A** to appear [hep-ph/0105311].
7. G. Aarts, J. Berges, hep-ph/0107129.
8. B. Mihaila, F. Cooper, J. F. Dawson, Phys. Rev. **D63** (2001) 096003 (2001).
9. K. Blagoev, F. Cooper, J. Dawson, B. Mihaila, hep-ph/0106195.
10. For improved results using inhomogeneous mean fields see G. Aarts, J. Smit, Phys. Rev. **D61** (2000) 025002; M. Sallé, J. Smit, J. C. Vink, Phys. Rev. **D64** (2001) 025016. L. M. Bettencourt, K. Pao, J. G. Sander-son, hep-ph/0104210.
11. For an early example see A. Ringwald, Phys. Rev. **D36** (1987) 2598.
12. L.M.A. Bettencourt, C. Wetterich, Phys. Lett. **B430** (1998) 140;
13. For studies in quantum mechanics see B. Mihaila, J. F. Dawson, F. Cooper, Phys. Rev. **D56** (1997) 5400; L. M. Bettencourt, C. Wetterich, hep-ph/9805360; B. Mihaila, T. Athan, F. Cooper, J. Dawson, S. Habib, Phys. Rev. **D62** (2000) 125015; A. V. Ryzhov, L. G. Yaffe, Phys. Rev. **D62** (2000) 125003.
14. S. Jeon, Phys. Rev. **D52** (1995) 3591; S. Jeon and L. Yaffe, Phys. Rev. **D53** (1996) 5799.
15. E.A. Calzetta, B.L. Hu, S.A. Ramsey, Phys. Rev. **D61** (2000) 125013.
16. L.P. Kadanoff, G. Baym, “Quantum Statistical Mechanics”, Benjamin, New York (1962).
17. P. Danielewicz, Ann. Phys. **152** (1984) 239; **197** (1990) 154;
18. S. Mrowczynski, P. Danielewicz, Nucl. Phys. **B342** (1990) 345; S. Mrowczynski and U. Heinz, Annals Phys. **229** (1994) 1.
19. J. Blaizot, E. Iancu, hep-ph/0101103.

20. Y. B. Ivanov, J. Knoll, D. N. Voskresensky, Nucl. Phys. **A672** (2000) 313; S. Leupold, Nucl. Phys. **A672** (2000) 475.
21. G. Aarts, G.F. Bonini, C. Wetterich, Phys. Rev. D **63** (2001) 025012.
22. F. Cooper, S. Habib, Y. Kluger, E. Mottola, J.P. Paz, P.R. Anderson, Phys. Rev. **D50** (1994) 2848; F. Cooper, S. Habib, Y. Kluger, E. Mottola, Phys. Rev. **D55** (1997) 6471.
23. D. Boyanovsky, H.J. de Vega, R. Holman, D.S. Lee, A. Singh, Phys. Rev. **D51** (1995) 4419; D. Boyanovsky, H.J. de Vega, R. Holman, J.F.J. Salgado, Phys. Rev. **D54** (1996) 7570; D. Boyanovsky, H. J. de Vega, R. Holman and J. Salgado, Phys. Rev. **D59** (1999) 125009;
24. J. Baacke, K. Heitmann and C. Pätzold, Phys. Rev. **D55** (1997) 2320, Phys. Rev. **D57** (1998) 6406; J. Baacke, S. Michalski, hep-ph/0109137.
25. D. Boyanovsky, C. Destri, H.J. de Vega, R. Holman, J. Salgado, Phys. Rev. **D57** (1998) 7388;
26. C. Wetterich, Phys. Rev. **E56** (1997) 2687 ; Phys. Rev. Lett. **78** (1997) 3598.
27. J. Schwinger, J. Math. Phys. **2** (1961) 407; L. V. Keldysh, Zh. Eksp. Teor. Fiz. **47** (1964) 1515 [Sov. Phys. JETP **20** (1965) 1018].
28. R.D. Pisarski, hep-ph/9710370; D. Boyanovsky, H.J. de Vega, R. Holman, S. Prem Kumar, R.D. Pisarski, Phys. Rev. **D57** (1998) 3653.
29. L. McLerran, R. Venugopalan, Phys. Rev. **D49** (1994) 2233; (1994) 3352; for a recent review see L. McLerran, hep-ph/0104285 and references therein; R.D. Pisarski, private communication.